(12) INTERNATIONAL APPLICATION PUBLISHED UNDER THE PATENT COOPERATION TREATY (PCT)

(19) World Intellectual Property Organization
International Bureau

(43) International Publication Date
19 August 2010 (19.08.2010)

PCT

(10) International Publication Number
WO 2010/094043 A2

(51) International Patent Classification:
A61K 49/18 (2006.01) *A61K 33/14* (2006.01)
A61K 49/10 (2006.01)

(21) International Application Number:
PCT/US2010/024324

(22) International Filing Date:
16 February 2010 (16.02.2010)

(25) Filing Language: English

(26) Publication Language: English

(30) Priority Data:
61/152,459 13 February 2009 (13.02.2009) US
61/162,989 24 March 2009 (24.03.2009) US

(71) Applicant *(for all designated States except US)*: **UNIVERSITY OF WASHINGTON** [US/US]; 4311 11th Avenue NE., Suite 500, Seattle, WA 98105-4608 (US).

(72) Inventors; and

(75) Inventors/Applicants *(for US only)*: **HO, Rodney, J.Y.** [US/US]; 3220 West Mercer Way, Mercer Island, WA 98040 (US). **HOEKMAN, John, D.** [US/US]; 303 Harvard Avenue, #204, Seattle, WA 98102 (US). **MARAVILLA, Ken** [US/US]; 11011 NE 12th, Unit 505, Bellevue, WA 98004 (US).

(74) Agent: **RENZONI, George, E.**; Christensen O'connor Johnson Kindness PLLC, 1420 Fifth Avenue, Suite 2800, Seattle, WA 98101 (US).

(81) Designated States *(unless otherwise indicated, for every kind of national protection available)*: AE, AG, AL, AM, AO, AT, AU, AZ, BA, BB, BG, BH, BR, BW, BY, BZ, CA, CH, CL, CN, CO, CR, CU, CZ, DE, DK, DM, DO, DZ, EC, EE, EG, ES, FI, GB, GD, GE, GH, GM, GT, HN, HR, HU, ID, IL, IN, IS, JP, KE, KG, KM, KN, KP, KR, KZ, LA, LC, LK, LR, LS, LT, LU, LY, MA, MD, ME, MG, MK, MN, MW, MX, MY, MZ, NA, NG, NI, NO, NZ, OM, PE, PG, PH, PL, PT, RO, RS, RU, SC, SD, SE, SG, SK, SL, SM, ST, SV, SY, TH, TJ, TM, TN, TR, TT, TZ, UA, UG, US, UZ, VC, VN, ZA, ZM, ZW.

(84) Designated States *(unless otherwise indicated, for every kind of regional protection available)*: ARIPO (BW, GH, GM, KE, LS, MW, MZ, NA, SD, SL, SZ, TZ, UG, ZM, ZW), Eurasian (AM, AZ, BY, KG, KZ, MD, RU, TJ, TM), European (AT, BE, BG, CH, CY, CZ, DE, DK, EE, ES, FI, FR, GB, GR, HR, HU, IE, IS, IT, LT, LU, LV, MC, MK, MT, NL, NO, PL, PT, RO, SE, SI, SK, SM, TR), OAPI (BF, BJ, CF, CG, CI, CM, GA, GN, GQ, GW, ML, MR, NE, SN, TD, TG).

[Continued on next page]

(54) Title: GADOLINIUM EXPRESSED LIPID NANOPARTICLES FOR MAGNETIC RESONANCE IMAGING

(57) Abstract: Lipid nanoparticles expressing metal ions and methods for using the compositions for magnetic resonance imaging.

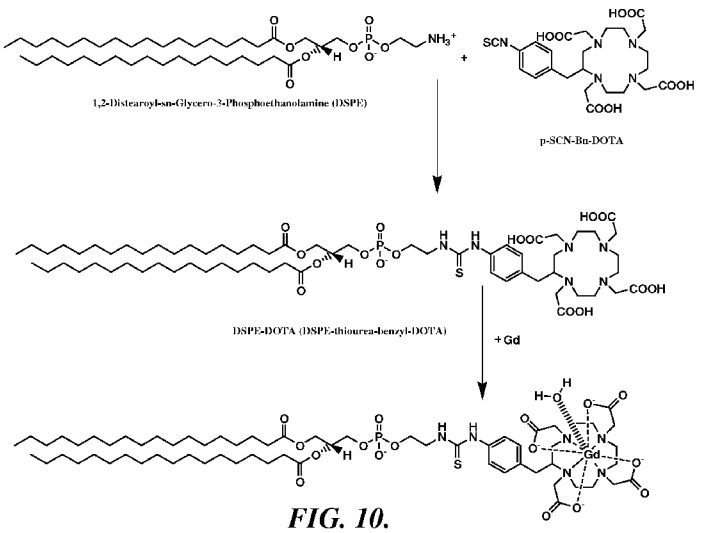

FIG. 10.

WO 2010/094043 A2

Published:

— *without international search report and to be republished upon receipt of that report (Rule 48.2(g))*

GADOLINIUM EXPRESSED LIPID NANOPARTICLES FOR MAGNETIC RESONANCE IMAGING

CROSS-REFERENCES TO RELATED APPLICATIONS

This application claims the benefit of U.S. Provisional Application No. 61/152,459, filed February 13, 2009, and U.S. Provisional Application No. 61/162,989, filed March 24, 2009. Each application is incorporated herein by reference in its entirety.

STATEMENT OF GOVERNMENT LICENSE RIGHTS

This invention was made with Government support under Contract No. AI 52663 awarded by the National Institutes for Health/National Institute of Allergy and Infectious Diseases. The Government has certain rights in the invention.

BACKGROUND OF THE INVENTION

Early diagnosis of lymph node involvement is essential to determine treatment for most types of cancer. Lymphadenectomy and histological evaluation is currently the gold standard, but is not ideal because it is invasive and can produce false negatives. Magnetic resonance (MR) imaging has become a powerful and non-invasive tool for detecting the spread of cancer to the lymph nodes. Standard MR imaging relies on size and morphology criteria to determine occult lymphoid tissues including lymph node metastasis, which has as low as 60% accuracy. MR contrast enhancing agents are becoming more widely used due to their usefulness in early tumor detection. Contrast enhancing agents diffuse into metastatic lymph nodes and healthy lymph nodes at different rates causing "filling defects." Predicting lymph node metastasis using filling defects from contrast agents as opposed to size criteria can increase the sensitivity from 29% to 93%.

Generally, there are two types of MR contrast enhancing agents. Superparamagnetic contrast agents have a low r2/r1 ratio and create dark spots in T2- and T2*-weighted images. These are usually based on iron oxide particles and are referred to as negative contrast agents. On the other hand, paramagnetic contrast agents increase the r1 relaxivity and have a high r2/r1 ratio, creating bright spots in T1 weighted MR images. These contrast agents are known as positive contrast agents and are usually complexes of gadolinium (Gd^{3+}).

T1 shortening comes about through dipole-dipole interactions with the protons in water so Gd^{3+}, with its seven unpaired electrons, is the optimal choice for a T1 relaxation

agent. Because Gd^{3+} is a heavy metal toxin, it is commonly delivered as a tightly bound linear or macroscopic chelate. Chelated forms of Gd^{3+} reduce toxicity by preventing cellular uptake of free Gd^{3+} and by limiting the clearance almost exclusively to renal filtration that resulted in renal toxicities. Despite reducing toxicity, the rapid clearance and small molecular size of gadolinium chelates mean that low levels of Gd^{3+} accumulates in the lymph nodes, making these agents a poor choice for MR lymphography. In addition, the FDA posted a warning about the risk of serious nephrogenic systemic fibrosis for all commercially available gadolinium contrast agent to identify well-perfused tissues and organs in subjects with acute or chronic renal insufficiency.

Liposomes and lipid nanoparticles containing Gd^{3+} have several advantages for MR contrast imaging of lymph nodes. Liposomes as well as lipid nanoparticles can lower the toxicity by encapsulating or binding to their surfaces a large amount of Gd^{3+}. However, the rapid clearance mechanism of intravenously (IV) administered liposomes does not significantly improve liposome-associated Gd^{3+} accumulation in the lymph nodes. Only a fraction of the lipid nanoparticles in blood are phagocytosed by reticuloendothelial cells, and only a fraction of those cells traverse to lymphatic system. Thus, IV administered liposomes provide indirect targeting of the lymphatic system and lymph nodes. However, this approach results in a majority of Gd^{3+} carrying liposomes eliminated through reticuloendothelial cells in blood. The pharmacokinetics of liposomes in blood can be optimized for lymph node accumulation through size and surface modification. Reducing the diameter of the liposomes below 200 nm decreases phagocytic dependent clearance and increases the circulation time in the blood. Adding polyethylene glycol (PEG, commonly referred to as PEGylation) to the liposome surface can also increase the circulation time and stability of liposomes.

Currently, gadolinium chelated with diethylenentriaminepentaacetyl (DTPA) provides contrast in magnetic resonance imaging to identify pathogenic tissues. Unfortunately, the soluble Gd-DTPA complexes approved for clinical use, such as OMNISCAN, are cleared within a few minutes and do not provide sufficient concentrations or time in lymphoid tissues. In addition, the residual fraction of gadolinium can lead to fibrosis in patients with renal insufficiency.

Despite the advances in the development of contrast agents, a need exists for improved contrast agents having longer *in vivo* life, provide sufficient concentration in

tissues to be analyzed, and low residual gadolinium concentrations to avoid side effects. The present invention seeks to fulfill this need and provide further related advantages.

SUMMARY OF THE INVENTION

The present inventions provides compositions expressing metal ions and methods for using the compositions.

In one aspect, the invention provides a composition, comprising a lipid, a polyalkylene-containing lipid, and a lipid-containing metal chelator.

Representative lipids include phospholipids, sphingolipids, cholesterol and steroid derivatives, bile acids and derivatives, cardilipin, acyl-glycerides and derivatives, glycolipids, acyl-peptides, fatty acids, carbohydrate-based polymers, functionalized silica, polyanhydride polymers, polylactate-glycolate polymers, and bioploymers. In one embodiment, the lipid is a phospholipid. Representative phospholipids include 1,2-distearoyl-sn-glycero-3-phosphocholine (DSPC); dipalmitoyl phosphatidylcholine; dimysristoyl phosphatidyl choline; dioleoyl phosphatidyl choline; trans-esterified phospholipids derived from eggs, soybean, flaxseed, and the like; and phosphatidylcholine substituted with phosphatidyl ethanolamine, phosphatidylglycerol, phosphatidyl serine, and phosphatidic acids.

Representative polyalkylene-containing lipids include polyoxyethylene-containing lipids or polyoxypropylene-containing lipids. In one embodiment, the polyalkylene-containing lipid is a phospholipid functionalized with polyethylene glycol such as N-(carbonyl-methoxypolyethyleneglycol-2000)-1,2-distearoyl-sn-glycero-3-phosphoethanol-amine (mPEG-2000-DSPE).

Representative lipid-containing metal chelators include 1,2-distearoyl-sn-glycero-3-phosphoethanolamine-N-diethylenetriaminepentaacetyl (DSPE-DTPA), tetraazacyclododecane, tetraacety(gadodiamide)-PE, and lipid-functionalized-[N,N-bis[2-[bis(carboxymethyl)amino]-ethyl]-glycinato-(5")]. In one embodiment, the lipid-containing metal chelator comprises a PEGylated lipid moiety. In one embodiment, the lipid-containing metal chelator is a PEGylated DTPA. In other embodiments, the lipid-containing metal chelator is a DSPE-BOPTA, a DSPE-DO3A, and a DSPE-DOTA.

In one embodiment, the composition further includes a targeting moiety. Representative targeting moieties include proteins, polypeptides, peptides, antibodies or fragments thereof, small molecules, sugars or polysaccharides or derivatives thereof, and nucleic acids.

In one embodiment, the composition of the invention has the form of a nanoparticle. In one embodiment, the nanoparticle has a diameter of from about 5 nm to about 2 μm. In one embodiment, the nanoparticle has a diameter of from about 50 nm to about 100 μm.

The composition of the invention can further include a metal ion. Suitable metal ions include paramagnetic metal ions and ions of radio-isotopes. Representative paramagnetic metal ions include Gd^{3+}, Cu^{2+}, Fe^{3+}, Fe^{2+}, and Mn^{2+} ions. Representative ions of radio-isotopes include ^{68}Ga, ^{55}Co, ^{86}Y, ^{90}Y, ^{177}Lu, and ^{111}In ions.

In another aspect, the invention provides administrable compositions including a carrier and a plurality of the nanoparticles of the invention. Suitable carriers include pharmaceutically acceptable carriers such as saline for injection or dextrose for injection.

In further aspect, the invention provides a method for imaging of tissues, comprising administering to a subject to be imaged an effective amount of the composition of the invention. Representative tissues that can be imaged by the method include lymphoid, cardiovascular, liver, kidney, brain, heart, muscle, and gastrointestinal tract tissues, and other tissues accessible by the lymphatic or vascular (blood) systems.

In another aspect, the invention provides a method for delivering a radio-cancer therapeutic agent to a cancer cell, comprising administering to a cancer cell an effective amount of the composition of the invention that includes anion of a radio-isotope.

DESCRIPTION OF THE DRAWINGS

The foregoing aspects and many of the attendant advantages of this invention will become more readily appreciated as the same become better understood by reference to the following detailed description, when taken in conjunction with the accompanying drawings.

FIGURE 1 is a graph illustrating reduction of calcein fluorescence as a function of Gd^{3+}: DTPA-PE (m/m) ratio for a representative formulation of the invention. The formulation was incubated with calcein and its fluorescence measured. Free Gd^{3+} binds to calcein and reduces its fluorescence.

FIGURES 2A and 2B compare relaxivity as a function of Gd^{3+} concentration. FIGURE 2A compares Gd^{3+} dose effect on T1 relaxation rate; R_1 (1/T1) values of Gd^{3+} concentrations (μmol/mL) measured in a 1.5T magnetic resonance (MR) scanner using a standard spin-echo sequence for a representative formulation of the invention (Gd-DPTA-PE: mPEG-PE: DSPC) compared to other formulations. FIGURE 2B compares Gd^{3+}

dose effect on T2 relaxation rate; R_2 (1/T2) values of Gd^{3+} concentrations (μmol/mL) measured in a 1.5T magnetic resonance (MR) scanner using a standard spin-echo sequence for a representative formulation of the invention (Gd-DPTA-PE: mPEG-PE: DSPC) compared to other formulations.

FIGURE 3 illustrates time-course coronal images of ventral cavity of *M. Nemestrina* up to 24 hours after injection of a representative formulation of the invention (Gd-DPTA-PE: mPEG-PE: DSPC). FIGURES 3A-3D are time sequence images of the liver before (3A) and after 20 min (3B), 6 hr (3C), and 24 hr (3D) administration. The top panel illustrates time sequence images of lymph nodes. The lymph nodes and liver show high contrast compared to background tissues.

FIGURE 4A is a graph comparing MR dynamic contrast enhanced image intensity of the lymph nodes (LN 1, LN 2, and LN3) and liver (Liver) in *M. Nemestrina* up to 24 hr after subcutaneous injection of 24.4 μmol/kg of a representative formulation of the invention (Gd-DPTA-PE: mPEG-PE: DSPC). Results are for images shown in FIGURES 3A-3D. FIGURE 4B is a graph comparing the time course of tissue specific MR signal (lymph node) compared to adjacent control tissue.

FIGURES 5A-5D are time course MR images of a rat after intravenous injection of a representative formulation of the invention (0.01 mmol/kg Gd-DPTA-PE: mPEG-PE: DSPC): pre-dose (5A); 5 min (5B); 14 min (5C); and 24 hr (5D). Contrast enhancement is localized mainly in vasculature and vascularized tissues in lymph nodes at 5 min and 14 min. The arrow in 5C indicates the beginning of gadolinium elimination into the gastrointestinal tract through the biliary route. By 24 hr (5D) most of the contrast agent is eliminated and the residual fraction appears in the intestine.

FIGURES 6A-6C are time course MR images of a rat after intravenous injection of a commercially available gadolinium-based contrast agent (0.05 mmol/kg Gd-DPTA, OMNISCAN): pre-dose (6A); 5 min (6B); and 15 min (6C). Contrast enhancement is diffused throughout and does not localize in the vasculature, well-perfused tissues, or the lymph nodes at either 5 min or 15 min. Distribution of contrast media to periphery and extremities is apparent.

FIGURES 7A-7D compare time course MR images of a rat after intravenous injection of a commercially available gadolinium-based contrast agent (0.05 mmol/kg Gd-DPTA, OMNISCAN, pre-dose (7A), 5 min (7B), and 15 min (7C)) an MR image of a

rat 15 min after administration of a representative formulation of the invention (0.01 mmol/kg Gd-DPTA-PE: mPEG-PE: DSPC).

FIGURES 8A-8F compare dose response MR images of a rat after intravenous injection of a representative formulation of the invention (Gd-DPTA-PE: mPEG-PE: DSPC): 0.0 mmol/kg (8A); 0.00125 mmol/kg (8B); 0.0025 mmol/kg (8C); 0.005 mmol/kg (8D); and 0.010 mmol/kg (8E and 8F). Lymph nodes are clearly apparent in FIGURE 8F.

FIGURES 9A-9C compare MR images of rats after intravenous injection of two commercially available gadolinium-based contrast agents (0.05 mmol/kg MS-325, 9A; 0.05 mmol/kg MAGNEVIST Gd-DPTA, 9B) and a representative formulation of the invention (0.01 mmol/kg Gd-DPTA-PE: mPEG-PE: DSPC, 9C). Images were acquired near peak enhancement, about 1 to 2 min after administration.

FIGURE 10 is a schematic illustration of the preparation of a representative lipid-containing gadolinium chelate: DSPE-DOTA-Gd.

FIGURE 11 illustrates three metal chelators useful for preparing representative lipid-containing chelates: p-SCN-Bn-DOTA; CHX-A"-DTPA; and p-SCN-Bn-DTPA.

FIGURE 12 is a schematic illustration of the preparation of representative lipid-containing gadolinium chelates.

DETAILED DESCRIPTION OF THE INVENTION

The present inventions provides compositions expressing metal ions and methods for using the compositions. In one embodiment, the compositions are lipid nanoparticles that include paramagnetic metal ions and are useful for magnetic resonance imaging. In another embodiment, the compositions are lipid nanoparticles that include ions of radio-isotopes and are useful for delivery of radio-cancer therapeutic agents.

In one aspect, the invention provides compositions and methods for magnetic resonance imaging. The compositions and methods enhance gadolinium distribution and accumulation in lymphatics. The invention provides a gadolinium composition (referred to herein as "Gd-DTPA-lipid nanoparticle") that is suitable for both intravenous and subcutaneous administration. Subcutaneous administration allows direct access to lymphatic system. The composition enhances T1 weighted MR signal in the lymph nodes as well as increases the residence time of the contrast agent in the lymphatics. Upon intravenous administration, the composition exhibits at least 100-fold enhancement over soluble Gd-DTPA as a vascular imaging agent and eliminates predominantly through

biliary, rather than renal clearance. The composition was shown to significantly increase signal-to-noise ratio by more than 300-fold for MR visualization of lymph nodes in macaques.

The composition of the invention includes a lipid, a polyalkylene-containing lipid, and a lipid-containing metal chelator. In one embodiment, the composition further includes a chelated metal ion.

In one embodiment, the composition of the invention is a chelator- (or metal chelate-) expressing particle. As used herein, the term "expressing" refers to the particle presenting or having available the chelator or chelated metal for activity. As noted above, in one embodiment, the composition of the invention is a lipid nanoparticle having chelated gadolinium ion (Gd^{+3}) (e.g., Gd-DTPA-lipid nanoparticle). In the lipid nanoparticle, chelated gadolinium ion is expressed.

The lipid nanoparticles of the invention are biocompatible and are readily administered. The nanoparticles have a diameter of from about 5 nm to about 2 μm. In one embodiment, the nanoparticles have a diameter of from about 10 nm to about 100 μm. In one embodiment, the nanoparticles have a diameter of about 70 nm.

As noted above, the composition of the invention (e.g., lipid nanoparticles) includes a lipid, a polyalkylene-containing lipid, and a lipid-containing metal chelator.

Lipids. The lipid component of the nanoparticles of the invention comprise the nanoparticle core.

Representative lipids useful in the compositions include phospholipids, sphingolipids, cholesterol and steroid derivatives, bile acids and derivatives, cardilipin, acyl-glycerides and derivatives, glycolipids, acyl-peptides, fatty acids, carbohydrate-based polymers (e.g., cellulose polymers), suitably functionalized silica, lipophilic polymers (e.g., polyanhydrides, polylactate-glycolate), and lipophilic bioploymers (e.g., proteins, sugar polymers).

In one embodiment, the lipid is disteroylamidomethylamine.

In one embodiment, the lipid is a phospholipid. Representative phospholipids include 1,2-distearoyl-sn-glycero-3-phosphocholine (DSPC); dipalmitoyl phosphatidylcholine; dimysristoyl phosphatidyl choline; dioleoyl phosphatidyl choline; trans-esterified phospholipids derived from eggs, soybean, flaxseed, and the like; and phosphatidylcholine substituted with phosphatidyl ethanolamine, phosphatidylglycerol,

phosphatidyl serine, and phosphatidic acids. In one embodiment, the phospholipid is 1,2-distearoyl-sn-glycero-3-phosphocholine (DSPC).

Polyalkylene-containing lipids. The polyalkylene-containing lipid component of the nanoparticles of the invention serve as surface hydrating agents.

Representative polyalkylene-containing lipids include polyoxyethylene-containing lipids and polyoxypropylene-containing lipids. In one embodiment, the polyalkylene-containing lipid is a phospholipid functionalized with polyethylene glycol (e.g., PEGylated phospholipid). Suitable PEGylated phospholipids include a polyethylene glycol having a number average molecular weight of from about 500 to about 20,000. In one embodiment, the PEGylated phospholipid is N-(carbonyl-methoxypolyethyleneglycol-2000)-1,2-distearoyl-sn-glycero-3-phosphoethanolamine (mPEG-2000-DSPE) (also referred to herein as "mPEG-DSPE" and "mPEG-PE").

In addition to polyalkylene-containing lipid, in other embodiments, the surface hydrating agent is hydrophilic biomaterials such as a carbohydrate polymer, a polyamine, a polyvinyl pyrrolidone, a poly(aspartate), or a poly(L-amino acid).

Other useful surface hydrating agents include covalent conjugates of polyethoxyl, polymethylene glycol, or propylene glycol and a lipid or other hydrophobic moiety (e.g., long chain hydrocarbon).

The surface hydrating agent is preferably present from about 5 to about 50 mole percent of the composition (i.e., lipid, polyalkylene-containing lipid (surface hydrating agent), and lipid-containing metal chelator).

Lipid-containing metal chelator. The lipid-containing metal chelator component of the nanoparticles of the invention are expressed on the surface of the nanoparticle and serve to chelate metal ions. Suitable lipid-containing metal chelators include two moieties: (1) a lipid moiety and (2) a metal chelator moiety.

Representative lipid-containing metal chelators include 1,2-distearoyl-sn-glycero-3-phosphoethanolamine-N-diethylenetriaminepentaacetyl (DSPE-DTPA), tetraazacyclododecane, tetraacety(gadodiamide or OMNISCAN)-PE, and lipid-functionalized-[N,N-bis[2-[bis(carboxymethyl)amino]ethyl]-glycinato-(5")] (MAGNEVIST).

Representative metal chelators include BOPTA, DO3A, and DOTA chelators.

In one embodiment, the metal chelator includes a PEGylated lipid moiety. Representative PEGylated metal chelators include DSPE-BOPTA, a DSPE-DO3A, and a

DSPE-DOTA. In one embodiment, the metal chelator is a PEGylated DTPA (DPTA-PE).

The metal chelator is preferably present from about 5 to about 50 mole percent of the lipid, polyalkylene-containing lipid (surface hydrating agent), and metal chelator.

Chelated metal ion. The compositions of the invention are effective carriers of metal ions. In these embodiments, the composition (e.g., lipid nanoparticles) further includes a chelated metal ion.

For MR applications, useful metal ions include paramagnetic metal ions. Representative paramagnetic metal ions include Gd^{3+}, Cu^{2+}, Fe^{3+}, Fe^{2+}, and Mn^{2+} ions.

For other applications such as imaging and therapeutic ion delivery, useful metal ions include ions of radio-isotopes. Representative radio-isotopes include ions of ^{68}Ga, ^{55}Co, ^{86}Y, ^{90}Y, ^{177}Lu, and ^{111}In.

For embodiments that include chelated metal ions, the ratio of metal ion: metal chelator is 0.1-1.0: 1.0 (less than or equal to 1:1).

Targeting agents. The compositions of the invention can be used to target specific tissues. In these embodiments, the composition (e.g., lipid nanoparticles) further includes a targeting moiety. Representative targeting moieties include proteins, polypeptide, and peptides; antibodies and derivatives (fragments); small molecules; sugars, polysaccharides, and derivatives; and nucleic acids, such as nucleotide polymers (e.g., aptamers), DNAs; and RNAs. Representative targeting moiety targets include cancer cells and virus infected cells.

Lipid nanoparticle formulations. The lipid nanoparticles of the invention can be formulated into compositions for administration. Suitable compositions for administration include a carrier and a plurality of the lipid nanoparticles. Representative carriers include pharmaceutically acceptable carriers, such as saline for injection or dextrose for injection.

The lipid nanoparticle of the invention is not a liposome and does not form liposomes when formulated.

Methods for tissue imaging. In another aspect, the invention provides methods for imaging tissues (e.g., occluded tissues). In one embodiment, the method includes administering to a subject to be imaged a diagnostically effective amount of a composition of the invention. The composition can be administered by a variety of techniques including subcutaneously and intravenously. The method is effective for

imaging tissues such as lymphoid, cardiovascular, liver, kidney, brain, heart, muscle, and gastrointestinal tract tissues, and other tissues accessible by the lymphatic or vascular (blood) systems. The method is effective for imaging the tissues above to determine whether the tissues are occluded. For magnetic resonance imaging methods, the composition includes a paramagnetic metal ion (e.g., Gd^{3+}).

In general, the effective amount is from about 0.001 to about 5 mmol metal/kg subject. In one embodiment, the effective amount is from about 0.005 to about 0.050 mmol metal/kg subject. In one embodiment, the effective amount is about 0.010 mmol metal/kg subject.

Methods for radio-cancer therapeutic agent delivery. In another aspect, the invention provides methods for delivering a radio-cancer therapeutic agent to a cancer cell. In one embodiment, the method includes administering to a subject in need thereof a therapeutically effective amount of a composition of the invention in which the chelated metal ion is a radio-isotope (e.g., ^{68}Ga, ^{55}Co, ^{86}Y, ^{90}Y, ^{177}Lu, and ^{111}In). The composition can be administered by a variety of techniques including subcutaneously and intravenously. The method is effective for delivery to tissues such as lymphoid, cardiovascular, liver, kidney, brain, heart, muscle, and gastrointestinal tract tissues, and other tissues accessible by the lymphatic or vascular (blood) systems.

The following is a description of the preparation, characterization, and imaging results for representative lipid nanoparticles of the invention.

Lipid nanoparticles were prepared composed of 10 mole percent of surface-bound DTPA. These lipid nanoparticles contained distearoyl-phosphatidylcholine and PEGylated lipid, mPEG-2000-DSPE. They were allowed to complex with Gd^{3+} (presented as $Gd^{3+}\cdot\cdot Cl^{-}$) at varying Gd^{3+}-to-DTPA-PE mole ratios. The presence of free Gd^{3+} in the admixture was determined by the ability of free Gd^{3+} to quench the fluorescence of calcein. With up to a Gd^{3+}-to-DTPA-PE mole ratio of 4, no free Gd^{3+} could be detected by the calcein quenching assay. At a 6 or higher Gd^{3+}-to-DTPA-PE mole ratio, free or unbound Gd^{3+} was detected (see FIGURE 1). To determine the effects of Gd^{3+} on DTPA-expressing lipid nanoparticles, we determined the particle diameter by photon correlation spectroscopy. The diameter of DTPA-expressing lipid nanoparticles was Gd^{3+} concentration dependent. At or below a Gd^{3+}-to-DTPA mole ratio of 1, the presence of Gd^{3+} did not influence the diameter of lipid nanoparticles. At a Gd^{3+}-to-DTPA mole ratio of 2, the apparent diameter of Gd^{3+}-DTPA lipid nanoparticle increases

by about 2- to 3-fold, while there is no apparent decrease in the degree of Gd associated with DTPA-lipid nanoparticles (see Table 1). These lipid nanoparticles appeared to be stable as no significant change in diameter was detected over 24 hr at room temperature. Collectively, these data suggest that the ratio of Gd^{3+}-to-DTPA influence the degree of Gd^{3+} incorporation into Gd-DTPA lipid nanoparticles and their apparent diameters. At or below Gd^{3+}-to-DTPA mole ratio of 2, substantially all Gd^{3+} was associated with lipid nanoparticles. In one embodiment, the Gd^{3+}-to-DTPA mole ratio in the composition of the invention is about 1.

The contrast properties of the Gd^{3+}-expressed lipid nanoparticles was determined by comparing the effects of the various Gd^{3+} formulations on the R1 (1/T1) relaxivity of Gd^{3+}. Lipid nanoparticles composed of distearoyl-phosphatidylcholine (DSPC) with or without PEGylated lipid (mPEG-2000-DSPE, referred to herein as "mPEG-DSPE" or "mPEG-PE") and fixed Gd^{3+}-to-DTPA mole ratio at 1. The T1 and T2 measurements were collected with a 1.5 T MR scanner. A clinically-used Gd-DTPA preparation (OMNISCAN, commercially available from GE Healthcare, Princeton, NJ) was included as a comparison. As shown in FIGURE 2A, the representative composition of the invention, Gd-DTPA lipid nanoparticle containing mPEG-PE (Gd-DTPA-PE: mPEG-PE: DSPC), exhibited significantly higher R1 value than other preparations, including OMNISCAN and lipid nanoparticles that did not contain mPEG. The effects of mPEG on Gd-DTPA lipid nanoparticles are less for T2 measurement (see FIGURE 2B). However, the R1 and R2 values for both Gd-DTPA lipid nanoparticle compositions (Gd-DTPA-PE: mPEG-PE: DSPC and Gd-DTPA-PE: DSPC) were significantly higher than that of the soluble Gd-DTPA commercial preparation (OMNISCAN) or free Gd^{3+} in solution (Gd w/o DTPA). To our knowledge the R1 values for Gd-DTPA nanoparticles of the invention are the highest value observed to date including those reported with Gd^{3+}-expressed liposome containing PEG. In fact these results were more than 10-fold higher than the data collected with Gd-DTPA liposomes containing egg lectin and cholesterol that express PEG (MW = 5000) linked to egg transesterified PE, instead of mPEG linked to DSPE.

Both of the nanoparticle formulations containing Gd^{3+} had higher R1 values than soluble Gd-DTPA. As expected, the DSPC and DSPC plus mPEG-2000-PE control formulations without Gd^{3+} showed no significant effect on relaxivity. The data indicates that the PEG-containing Gd-DTPA-lipid nanoparticles provide a much greater increase in

R1 compared to the other formulations. Up to a 100-fold increase in R1 relaxivity was achieved when compared to the commercially available OMNISCAN. The Gd-DTPA nanoparticle formulation without surface PEG (Gd-DTPA-PE: DSPC) also showed higher R1 values than OMNISCAN, but much less than the PEG-containing Gd-DTPA-lipid nanoparticle formulation (Gd-DTPA-PE: mPEG-PE: DSPC) (see FIGURE 2A).

Because positive contrast generated by Gd^{3+} in an MR image is dependant on a low R2/R1 ratio, changes of R2 values were also determined. FIGURE 2B demonstrates the effects of the various Gd^{3+} formulations on the R2 (1/T2) relaxivity measurements. Once again the PEGylated Gd-DTPA-lipid nanoparticles (Gd-DTPA-PE: mPEG-PE: DSPC and Gd-DTPA-PE: DSPC) showed a greater increase in R2 compared to the other formulas, however the magnitude of the change was less. The mPEGylated Gd-DTPA-lipid nanoparticles (Gd-DTPA-PE: mPEG-PE: DSPC) showed about eight-fold increase in R2, compared to OMNISCAN. The Gd-DTPA in DSPC (without mPEG) nanoparticle formulation (Gd-DTPA-PE: DSPC) showed a greater increase in R2 than R1, which may limit its effectiveness as a positive contrast agent formulation. The DSPC and DSPC plus mPEG-2000-PE control formulations without Gd^{3+} (DTPA-PE: mPEG-PE: DSPC and DTPA-PE: DSPC) again showed no effect on relaxivity. The relaxivity experiments show that the mPEGylated Gd-DTPA-lipid nanoparticle formulation greatly increases the R1 relaxivity compared to other formulations. However, at high concentrations (greater than 3 μmol/ml), the T1 spillover into T2 becomes significant, leading to an apparent reduction of T1 signal (data not shown). Optimal T1 tissue contrast could be obtained with minimum Gd^{3+} concentration. These data clearly demonstrate much higher contrast "potency" than that provided by the commercial product, OMNISCAN.

The use of the Gd-DTPA lipid nanoparticles containing mPEG-2000-PE (Gd-DTPA-PE: mPEG-PE: DSPC or "Gd-DTPA lipid nanoparticles") for MR imaging studies in primates is described below.

FIGURES 3A-3D shows several coronal MR images of ventral cavity of *M. Nemestrina* both pre-contrast and up to 24 hours following subcutaneous injection of Gd^{3+}-DTPA-lipid nanoparticles. The auxiliary lymph nodes are clearly visible with a high degree of intensity enhancement compared to the surrounding tissue (FIGURE 3 top panel). The enhancement of the lymph nodes can be seen as early as twenty minutes while lasting up to twenty four hours. FIGURE 4 shows the time course of dynamic contrast enhanced MRI, showing relative intensities of various organs vs. time. This data

shows that the Gd^{3+}-DTPA-lipid nanoparticles quickly reach the lymph nodes tissue within twenty minutes after injection, and maintain the contrast enhancement for at least twenty four hours. Compared to a low signal that dissipates within 20 min in lymphatic system of animals treated intravenously with soluble Gd-DTPA (OMNISCAN preparations), a single subcutaneous Gd-DTPA lipid nanoparticles dose provided greatly enhanced signal for extended time.

The MR image enhancing property of the Gd-DTPA-lipid nanoparticles can be used to minimize the IV dose need to produce vascular image enhancement and also reduce renal burden. Administration of 0.01 mmole/kg Gd-DTPA nanoparticles (about 1/5 of current dose for human) in rats produced a high quality MR image with clearly discernable central and peripheral vasculature of rat within 5 min (FIGURE 5B). It begins to clear through the bile and gut within 15 min (FIGURE 5C), and by the clearance process appeared to complete by 24 hr (FIGURE 5D). In contrast, 0.05 mmole soluble Gd-DTPA (OMNISCAN) produce diffuse contrast localization with no vascular definition; it also appeared to distribute to periphery an extremities (FIGURES 6A). In a limited dose-response study, only about to 10-20-fold lower dose of the Gd-DTPA-lipid nanoparticles, compared to current Gd-DTPA formulation, is needed in rat to produce equivalent or better definition of contrast enhanced MR images in rats. The 0.0025 mmole/kg Gd in DTPA-lipid nanoparticles produce equivalent image quality of 0.05 mmole/kg Gd-DTPA (OMNISCAN) preparation. Therefore, the Gd-DTPA-lipid nanoparticles may overcome challenges in the clinical use with currently approve Gd contrast agents due to renal insufficiency and neurotoxicity.

The PEGylated lipid nanoparticles of the invention having surface-bound gadolinium ion exhibited a great improvement over other preparations in contrast enhanced MR lymphography and vascular imaging. These lipid nanoparticles showed high degree of accumulation in the lymph nodes after subcutaneous injection. The contrast enhancement in lymphoid tissue begins within 20 minutes of injection and is maintained for 24 hours. When given intravenously this agent produced high quality images of vasculature in much higher sensitivity than the current agents. Intravenously administered lipid nanoparticles are cleared almost exclusively through biliary route and appeared to complete within 24 hr. Surface modification by adding mPEG in lipid nanoparticles increased the MR signal of Gd^{3+} through coordination of water molecules. This leads to a much higher R1 relaxivity and lymph node image enhancement. The lipid

nanoparticle formulation may allow using a low dose to achieve a high signal-to-noise MR contrast ratio for increasing the metastatic nodal discrimination and allowing for a much wider time frame for imaging. The potentially lower dose and more favorable elimination route of Gd^{3+} needed for MR contrast could provide higher safety margin.

The formulations of the invention provide effective contrast at relatively low dose compared to currently available and approved contrast agents. FIGURES 8A-8F compare dose response MR images of a rat after intravenous injection of a representative formulation of the invention (Gd-DPTA-PE: mPEG-PE: DSPC): 0.0 mmol/kg (8A); 0.00125 mmol/kg (8B); 0.0025 mmol/kg (8C); 0.005 mmol/kg (8D); and 0.010 mmol/kg (8E and 8F). Lymph nodes are clearly apparent in FIGURE 8F.

As noted above, the formulations of the invention offer advantages over currently available and approved contrast agents. FIGURES 9A-9C compare MR images of rats after intravenous injection of two commercially available gadolinium-based contrast agents (0.05 mmol/kg MS-325, EPIX Pharmaceuticals, Inc., Cambridge, MA, FIGURE 9A; and 0.05 mmol/kg MAGNEVIST Gd-DPTA, Bayer HealthCare Pharmaceuticals, FIGURE 9B) and a representative formulation of the invention (0.01 mmol/kg Gd-DPTA-PE: mPEG-PE: DSPC, FIGURE 9C). Images were acquired near peak enhancement, about 1 to 2 min after administration. As can be seen from the images, the representative formulation of the invention demonstrates significantly greater contrast than the currently available agents.

FIGURE 10 is a synthetic scheme for preparing a representative Gd complexes useful in the invention (DSPE-DOTA-Gd) by reacting DSPE with p-SCN-Bn-DOTA followed by Gd metallation. FIGURE 11 illustrates three representative chelating agents (isothiocyanates, -N=C=S or -NCS) (p-SCN-Bn-DOTA, CHX-A"-DTPA, and p-SCN-Bn-DTPA) that are reactive toward phospholipids and useful in the invention. FIGURE 12 illustrates four representative lipophilic compounds (DSA, Diether PE, DSPE-PEG(2000) Amine, and DSPE) and a synthetic scheme for preparing a representative Gd complex useful in the invention (DSPE-DOTA-Gd) by reacting DSPE with p-SCN-Bn-DOTA followed by Gd metallation. Lipid-containing metal chelators useful in the invention are readily prepared as shown in FIGURES 10 and 12. Suitably reactive metal chelators (e.g., isothiocyanate-functionalized metal chelators, see FIGURE 11) are reacted with lipid compounds containing suitably reactive groups (e.g., amino groups in DSPE, DSPE-PEG(2000) Amine, Diether PE, DSA, see FIGURES 10 and 12) to provide

lipid-containing metal chelators in which the lipid moiety is covalently coupled to the metal chelator. For isothiocyanate-functionalized metal chelators and reactive amine-containing lipids, the product lipid-containing metal chelator includes a thiourea (-NH-C(=S)-NH-) linkage coupling the lipid to the chelator. It will be appreciated that other suitably reactive metal chelators (e.g., isocyanate) and lipid compounds containing suitably reactive groups (e.g., alcohol) can provide lipid-containing metal chelators useful in the invention. Metallation of the chelators provides the metal ion-containing compounds.

Table 1: Effects of the Gd^{3+} to DTPA mole ratio on particle size and stability of Gd^{3+}-lipid nanoparticles[a].

Gd^{3+}: DTPA (m/m) ratio[b]	Particle diameter (nm)[c]		Free or unbound Gd^{3+} [d]
	After preparation	At 24 hr	
0	52±0.05	65±0.3	--
0.5	46±0.09	49±0.07	1.4 ± 2.7%
1	41±0.1	48±0.1	1.6 ± 4.8%
2	137±0.15	145±0.2	0.8 ± 2.0%

[a]DTPA is expressed on lipid nanoparticles composed of DSPC, mPEG-PE and DTPA-PE (8:1:0.9 mole ratio, as described in Example 1.

[b]The nanoparticles were exposed to $GdCl_3$ at indicated DTPA to Gd^{3+} mole ratio.

[c]The diameter of DTPA expressed nanoparticles were measured by photon correlation spectroscopy and data expressed were mean ± SD of quadruplicate samples at indicated time points.

[d]The presence of unbound or free Gd^{3+} was estimated with calcein fluorescence quenching assay.

The following examples are provided for the purpose of illustrating, not limiting, the invention.

Examples

Example 1

Materials and Methods

Lipid nanoparticle preparation. 1,2-distearoyl-sn-glycero-3-phosphocholine (DSPC, Avanti Polar Lipids, AL), N-(carbonyl-methoxypolethyleneglycol-2000)-1,2-distearoyl-sn-glycero-3-phospoethanolamine (mPEG-2000-DSPE, Genzyme, MA), and 1,2- distearoyl-sn-glycero-3-phophoethanolamine-N-DTPA (DSPE-DTPA, Avanti Polar Lipids, AL) were combined in chloroform (DSPC: mPEG-DSPE: DSPE-DTPA) in a ratio of 8:2:1 and dried into a thin film under nitrogen and then under high vacuum overnight. The mPEG-DSPE containing PEG polymers of various molecular weights (or chain lengths) are also purchased from Genzyme, MA. At this point phosphate buffered saline (PBS, pH 7.4) was added to the film and sonicated in a bath-type sonicator (Laboratory Supplies Company, New York). The vesicle diameter, as measured by dynamic light scattering using a Malvern Zetasizer 5000 photon correlation spectroscopy (Malvern Instruments, PA), was 50 nm. The nanoparticles in suspension were mixed with gadolinium (III) chloride hexahydrate (Aldrich, St Louis, MO) for 20 minutes at indicated mole ratio to form Gd-DTPA-lipid nanoparticles. To determine the unbound Gd^{3+}, the nanoparticles were incubated with calcein (0.5 μM) (Sigma, St Louis, MO) in PBS, pH 7.4, and the fluorescence was measured at 485/535 nm using a Victor3V 1420 multilabel counter (PerkinElmer, Waltham, MA). Free ionic Gd^{3+} quenches calcein fluorescence in $[Gd^{3+}]$ dependent manner. To determine the final Gd concentration, elemental Gd mass was determined using the inductively coupled plasma atomic emission spectrometry. The particles along with control particles without Gd^{3+} were used in the studies described herein.

Relaxivity studies. Dilutions of Gd-DTPA-lipid nanoparticles were prepared with Gd^{3+} concentrations between 0-5 μmol/ml. For comparison several samples were prepared from commercial agents such as OMNISCAN (Gd-DTPA-BMA) with Gd^{3+} concentrations from 0-5 μmol/ml. The relaxation time T1 was measured using the standard spin-echo sequence on a 1.5T MR scanner with a volume head coil as RF receiver. For T1 measurements, TE was fixed to 9 ms and seven TR were 133, 200, 300, 500, 750, 1000 and 2000 ms, respectively. For T2 measurements, TR was fixed to 2000 ms and four TE were 15, 30, 45, and 60 ms, respectively. The imaging intensities were

fitted to obtain the corresponding T1 and T2 values, which were plotted versus Gd^{3+} concentration.

Primate lymphatic MRI Study. *In vivo* imaging of the lymph nodes using Gd-DTPA-lipid nanoparticles for dynamic contrast enhanced (DCE) MRI was performed in a 1.5T MR scanner. The pigtailed macaque (*M. Nemestrina*) was anesthetized with inhaled isofluorane (1-2%) and closely monitored during the experiments. A pre-contrast image of the primate was recorded to determine proper lymph node location and fine-tune the imaging parameters. The animal was removed from the MR scanner and injected subcutaneously at four sites. Each injection site received 2, 5, 5, and 8.5 mL, respectively of 6.1 μmol/ml Gd-DTPA-lipid nanoparticles to allow probing of dose effects and contrast diffusion from injection sites. The total dose of Gd is estimated to be 24.4 μmol/kg for the primate studies. The images were recorded on a Signa 1.5T Scanner using a surface coil 12 x 12 $inch^2$. A standard spin-echo imaging sequence was used with TR=500 ms, TE = 15 ms, slice thickness of 3 mm, 21 slices, slice gap = 0.5 mm, FOV (field of view) = 320 x 320 mm^2, matrix size = 512 x 512, which gives an in-plane resolution of 0.63 x 0.63 mm^2 and a temporal resolution is 3.1 min.

Rat vascular MRI study. *In vivo* imaging of the rat using Gd-DTPA-lipid nanoparticles for dynamic contrast enhanced (DCE) MRI was performed in a 3.0T MR scanner. The rats (SD) was anesthetized with inhaled isofluorane (1-2%) and closely monitored during the experiments. A pre-contrast image of the rat was recorded to determine proper location, orientation and fine-tune the imaging parameters. The animal was removed from the MR scanner and injected with 400 μL of indicated Gd contrast media through femoral vein. The images were recorded on a Signa 1.5T Scanner using a surface coil 12 x 12 inch. A standard spin-echo imaging sequence was used with TR=500 ms, TE = 15 ms, slice thickness of 3 mm, 21 slices, slice gap = 0.5 mm, FOV (field of view) = 320 x 320 mm^2, matrix size = 512 x 512, which gives an in-plane resolution of 0.63 x 0.63 mm^2 and a temporal resolution is 3.1 min.

While the preferred embodiment of the invention has been illustrated and described, it will be appreciated that various changes can be made therein without departing from the spirit and scope of the invention.

CLAIMS

The embodiments of the invention in which an exclusive property or privilege is claimed are defined as follows:

1. A composition, comprising:
   (a) a lipid;
   (b) a polyalkylene-containing lipid; and
   (c) a lipid-containing metal chelator.

2. The composition of Claim 1, wherein the lipid is selected from the group consisting of phospholipids, sphingolipids, cholesterol and steroid derivatives, bile acids and derivatives, cardilipin, acyl-glycerides and derivatives, glycolipids, acyl-peptides, fatty acids, carbohydrate-based polymers, functionalized silica, polyanhydride polymers, polylactate-glycolate polymers, and bioploymers.

3. The composition of Claim 1, wherein the lipid is a phospholipid.

4. The composition of Claim 3, wherein the phospholipid is selected from the group consisting of 1,2-distearoyl-sn-glycero-3-phosphocholine (DSPC); dipalmitoyl phosphatidylcholine; dimysristoyl phosphatidyl choline; dioleoyl phosphatidyl choline; trans-esterified phospholipids derived from eggs, soybean, flaxseed, and the like; and phosphatidylcholine substituted with phosphatidyl ethanolamine, phosphatidylglycerol, phosphatidyl serine, and phosphatidic acids.

5. The composition of Claim 1, wherein the polyalkylene-containing lipid is selected from the group consisting of polyoxyethylene-containing lipids and polyoxypropylene-containing lipids.

6. The composition of Claim 1, wherein the polyalkylene-containing lipid is a phospholipid functionalized with polyethylene glycol.

7. The composition of Claim 6, wherein the phospholipid functionalized with polyethylene glycol comprises a polyethylene glycol having a number average molecular weight from about 500 to about 20,000.

8. The composition of Claim 7, wherein the phospholipid functionalized with polyethylene glycol is N-(carbonyl-methoxypolyethyleneglycol-2000)-1,2-distearoyl-sn-glycero-3-phosphoethanolamine (mPEG-2000-DSPE).

9. The composition of Claim 1, wherein the lipid-containing metal chelator is selected from the group consisting of 1,2-distearoyl-sn-glycero-3-phosphoethanolamine-N-diethylenetriaminepentaacetyl (DSPE-DTPA), tetraazacyclododecane, tetraacety(gadodiamide)-PE, lipid-functionalized-[N,N-bis[2-[bis(carboxymethyl)amino]-ethyl]-glycinato-(5")].

10. The composition of Claim 1, wherein the lipid-containing metal chelator comprises a PEGylated lipid moiety.

11. The composition of Claim 1, wherein the lipid-containing metal chelator is a PEGylated DTPA.

12. The composition of Claim 1, wherein the lipid-containing metal chelator is selected from the group consisting of a DSPE-BOPTA, a DSPE-DO3A, and a DSPE-DOTA.

13. The composition of Claim 1, wherein the polyalkylene-containing lipid is present from about 5 to about 50 mole percent of the lipid, the polyalkylene-containing lipid, and lipid-containing metal chelator.

14. The composition of Claim 1, wherein the lipid-containing metal chelator is present from about 5 to about 50 mole percent of the lipid, the polyalkylene-containing lipid, and lipid-containing metal chelator.

15. The composition of any one of Claims 1-14 further comprising a targeting moiety.

16. The composition of Claim 15, wherein the targeting moiety is selected from the group consisting of a protein, a polypeptide, a peptide, an antibody or fragment thereof, a small molecule, a sugar or polysaccharide or derivative thereof, and a nucleic acid.

17. The composition of Claim 15, wherein the targeting moiety targets cancer cells or virus infected cells.

18. The composition of any one of Claims 1-17 in the form of a nanoparticle.

19. The composition of Claim 18, wherein the nanoparticle has a diameter of from about 5 nm to about 2 μm.

20. The composition of Claim 18, wherein the nanoparticle has a diameter of from about 50 nm to about 100 μm.

21. The composition of any one of Claims 1-20 further comprising a chelated metal ion.

22. The composition of Claim 21, wherein the ratio of chelated metal ion: metal chelator is 0.1-1.0:1.0.

23. The composition of Claims 21 or 22, wherein the chelated metal ion is a paramagnetic metal ion.

24. The composition of Claim 23, wherein the paramagnetic metal ion is selected from the group consisting of Gd^{3+}, Cu^{2+}, Fe^{3+}, Fe^{2+}, and Mn^{2+}.

25. The composition of Claims 21 or 22, wherein the chelated metal ion is an ion of a radio-isotope.

26. The composition of Claim 25, wherein the ion of a radio-isotope is selected from the group consisting of ions of ^{68}Ga, ^{55}Co, ^{86}Y, ^{90}Y, ^{177}Lu, and ^{111}In.

27. A composition, comprising a carrier and a plurality of the nanoparticles of Claim 18.

28. The composition of Claim 27, wherein the carrier is a pharmaceutically acceptable carrier.

29. The composition of Claim 27, wherein the carrier is saline for injection or dextrose for injection.

30. A method for imaging of tissues, comprising administering to a subject to be imaged an effective amount of the composition of any one of Claims 21-29.

31. The method of Claim 30, wherein the composition is administered subcutaneously.

32. The method of Claim 30, wherein the composition is administered intravenously.

33. The method of Claim 30, wherein the tissue is selected from the group consisting of lymphoid, cardiovascular, liver, kidney, brain, heart, muscle, and gastrointestinal tract tissues, and other tissues accessible by the lymphatic or vascular (blood) systems.

34. The method of Claim 30, wherein the effective amount is from about 0.001 to about 5 mmol metal/kg subject.

35. The method of Claim 30, wherein the effective amount is from about 0.005 to about 0.050 mmol paramagnetic metal/kg subject.

36. The method of Claim 30, wherein the effective amount is about 0.01 mmol paramagnetic metal/kg subject.

37. A method for delivering a radio-cancer therapeutic agent to a cancer cell, comprising administering to a cancer cell an effective amount of the composition of Claims 25 or 26.

38. The method of Claim 37, wherein the composition is administered subcutaneously.

39. The method of Claim 37, wherein the composition is administered intravenously.

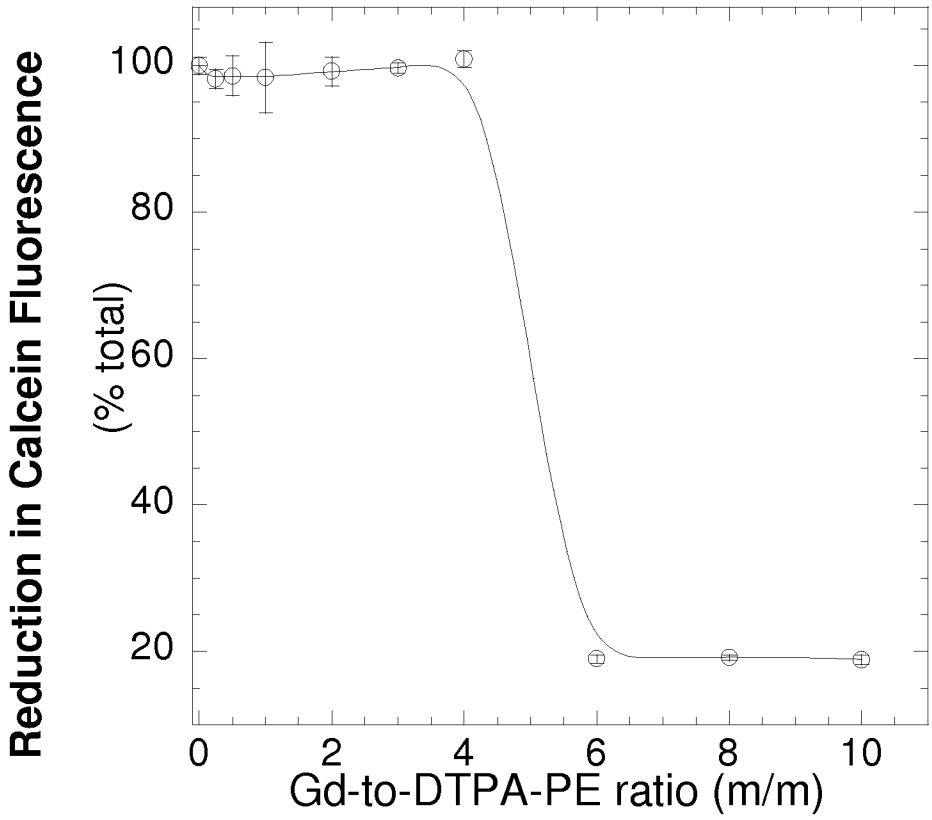
Reduction in Calcein Fluorescence
(% total)
100
80
60
40
20
0
2
4
6
8
10
Gd-to-DTPA-PE ratio (m/m)

FIG. 1.

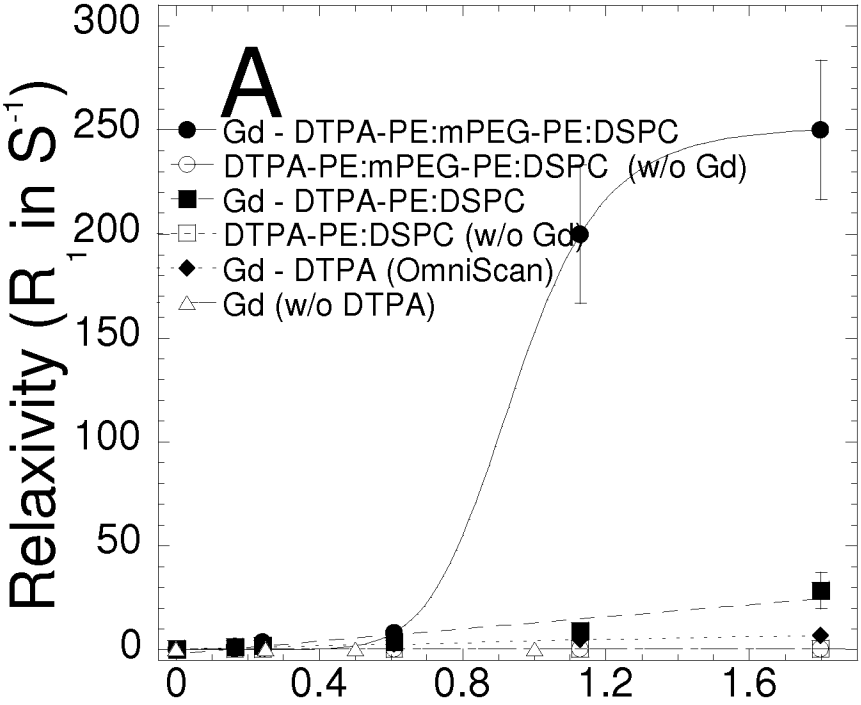
A
Gd - DTPA-PE:mPEG-PE:DSPC
DTPA-PE:mPEG-PE:DSPC (w/o Gd)
Gd - DTPA-PE:DSPC
DTPA-PE:DSPC (w/o Gd)
Gd - DTPA (OmniScan)
Gd (w/o DTPA)
Relaxivity (R_1 in S^{-1})
300
250
200
150
100
50
0
0
0.4
0.8
1.2
1.6

FIG. 2A.

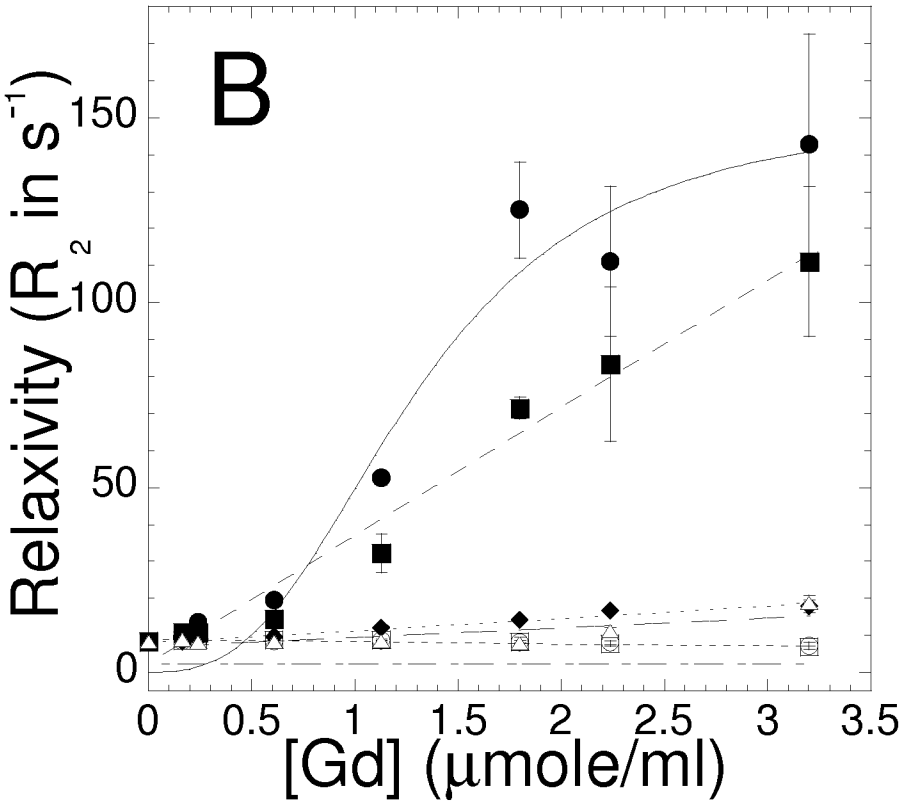
B
Relaxivity (R_2 in s^{-1})
150
100
50
0
0
0.5
1
1.5
2
2.5
3
3.5
[Gd] (μmole/ml)

FIG. 2B.

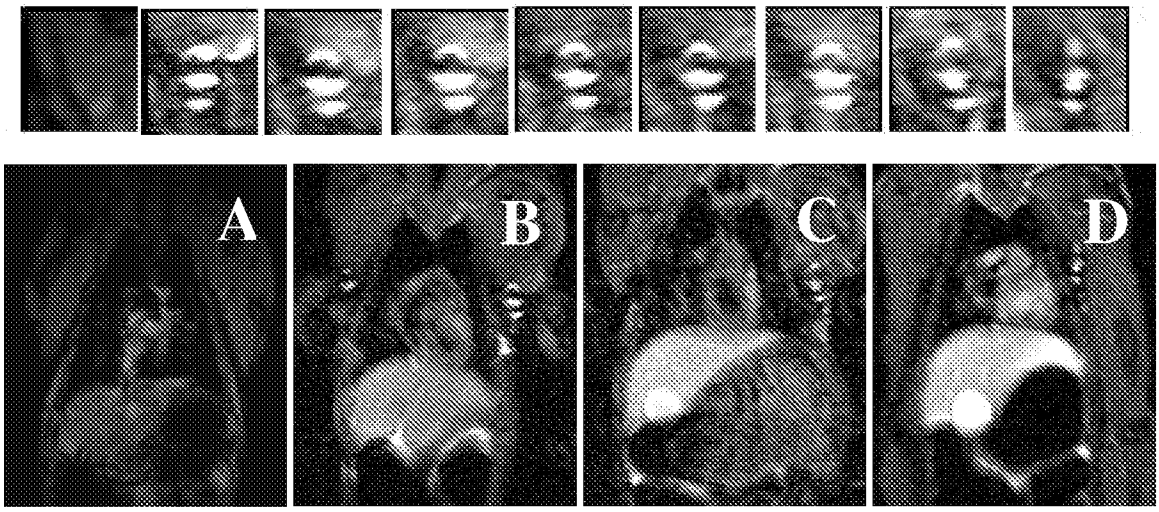

FIGS. 3A-3D.

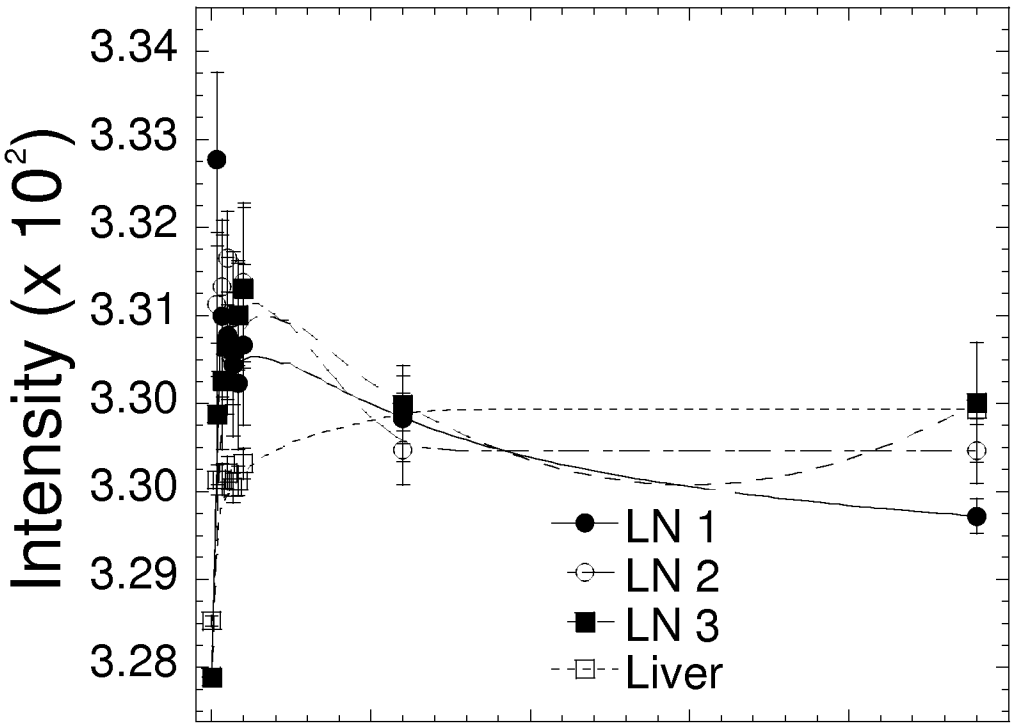
Intensity (x 10^2)
3.34
3.33
3.32
3.31
3.30
3.30
3.29
3.28
LN 1
LN 2
LN 3
Liver

FIG. 4A.

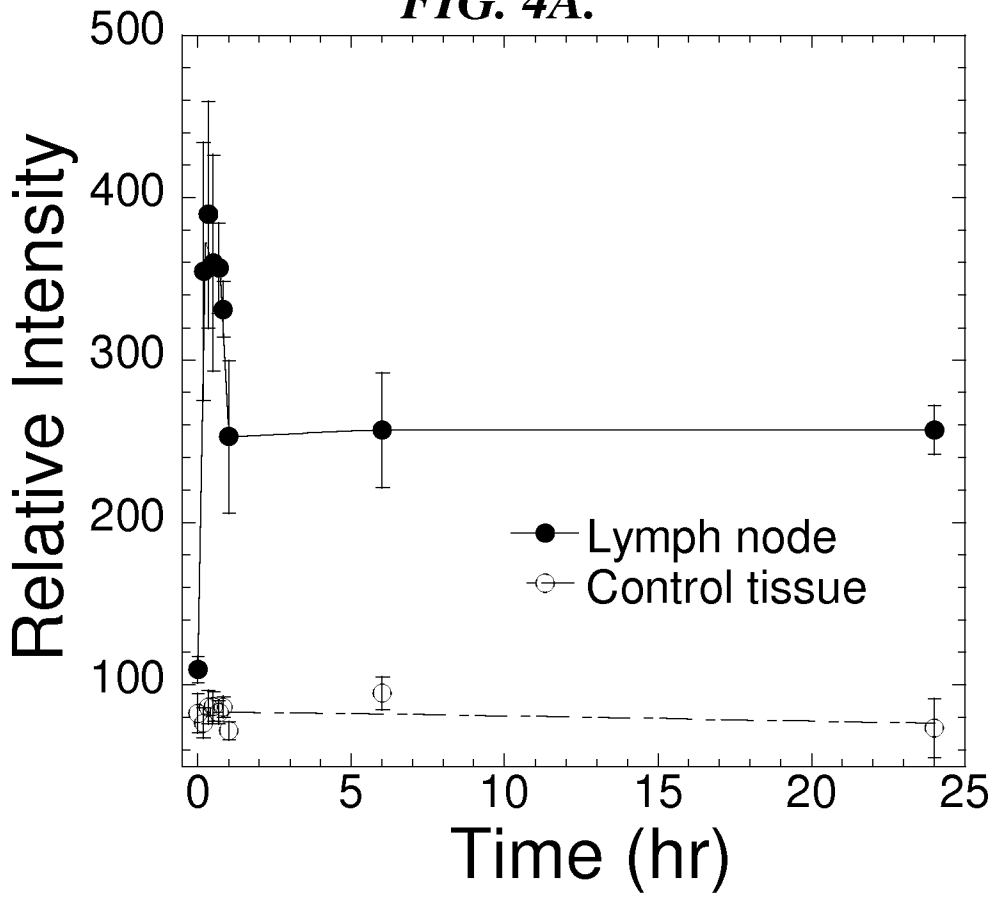
Relative Intensity
500
400
300
200
100
0
5
10
15
20
25
Time (hr)
Lymph node
Control tissue

FIG. 4B.

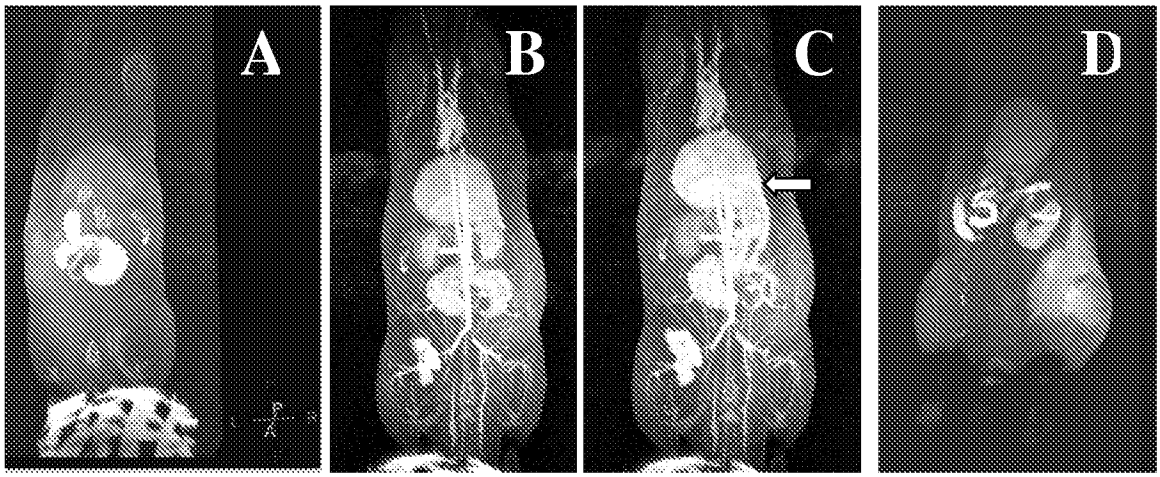

FIGS. 5A-5D.

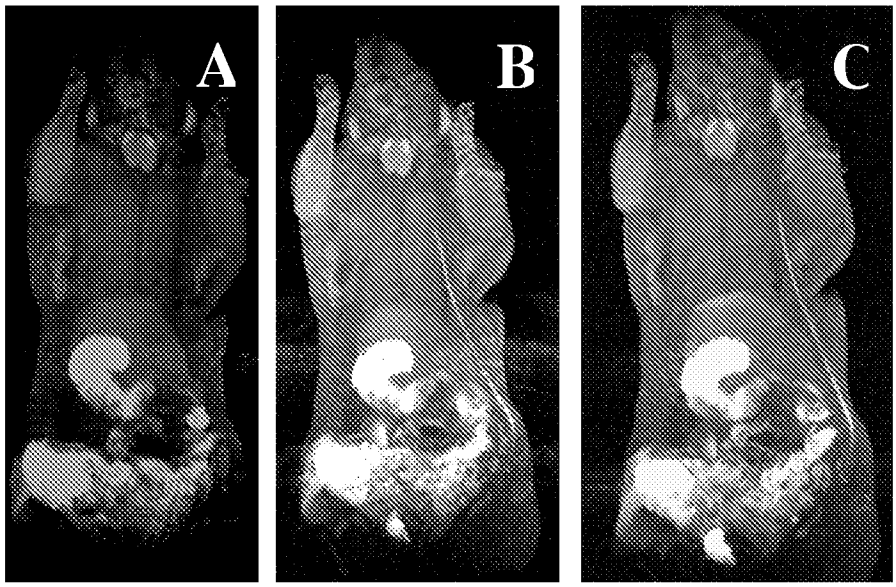

FIGS. 6A-6C.

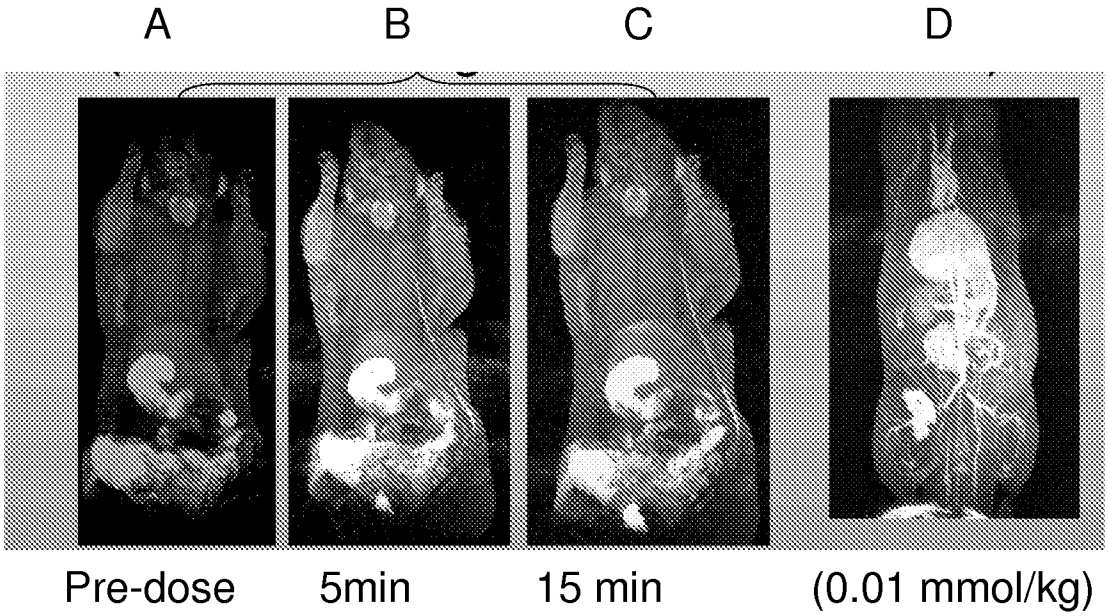

FIGS. 7A-7D.

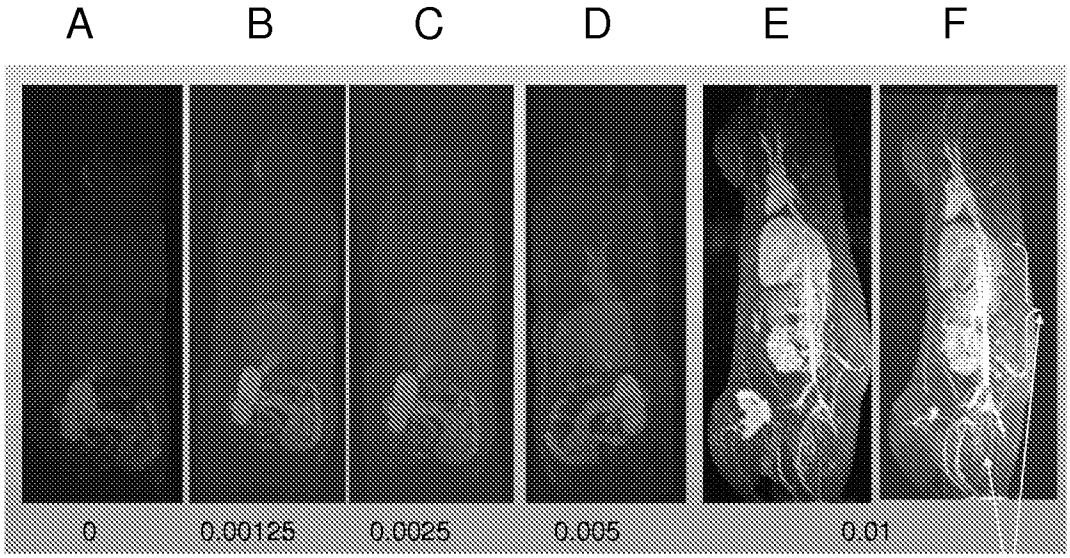

FIGS. 8A-8F.

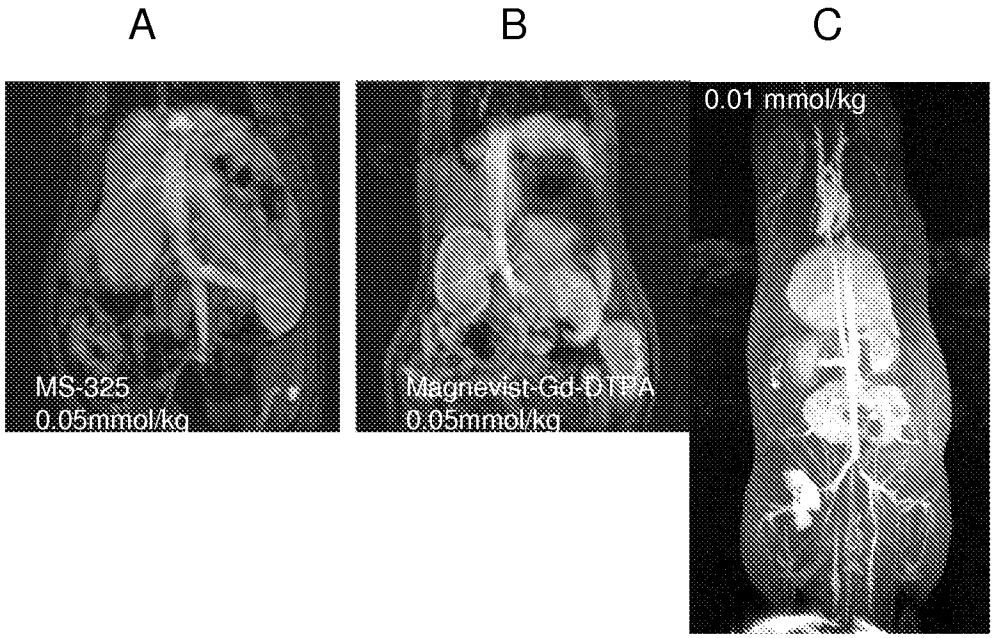
A
B
C
MS-325
0.05mmol/kg
Magnevist-Gd-DTPA
0.05mmol/kg
0.01 mmol/kg

FIGS. 9A-9C.

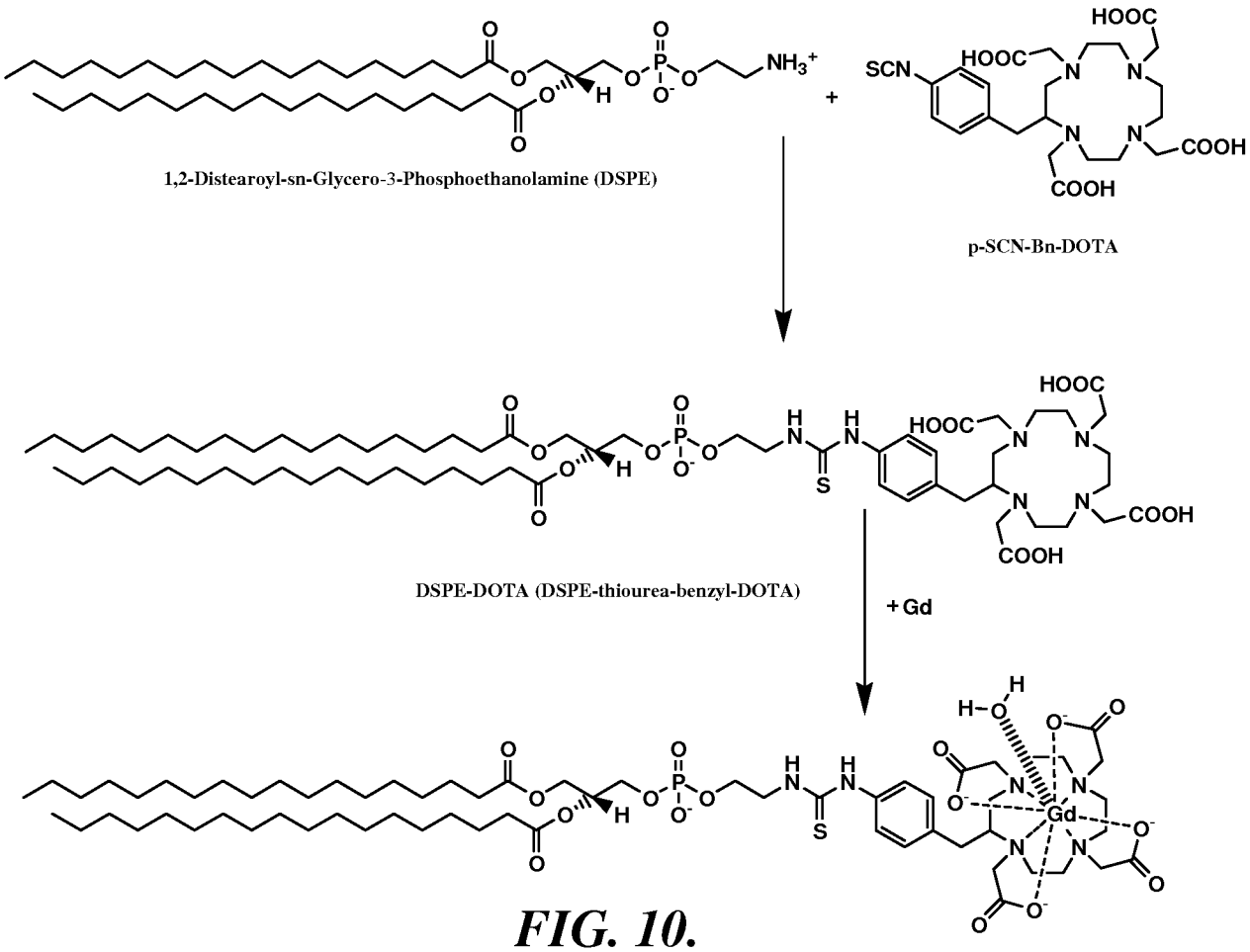
1,2-Distearoyl-sn-Glycero-3-Phosphoethanolamine (DSPE)
p-SCN-Bn-DOTA
DSPE-DOTA (DSPE-thiourea-benzyl-DOTA)
+ Gd

FIG. 10.

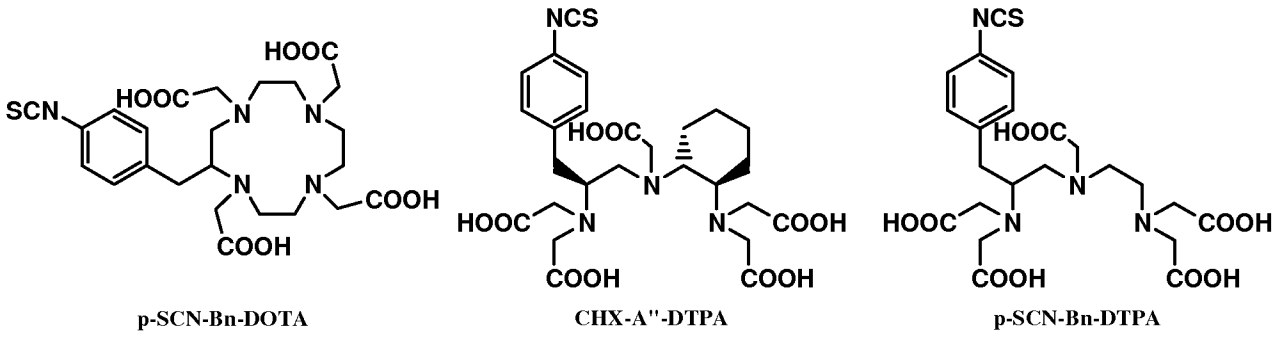
p-SCN-Bn-DOTA
CHX-A''-DTPA
p-SCN-Bn-DTPA

FIG. 11.

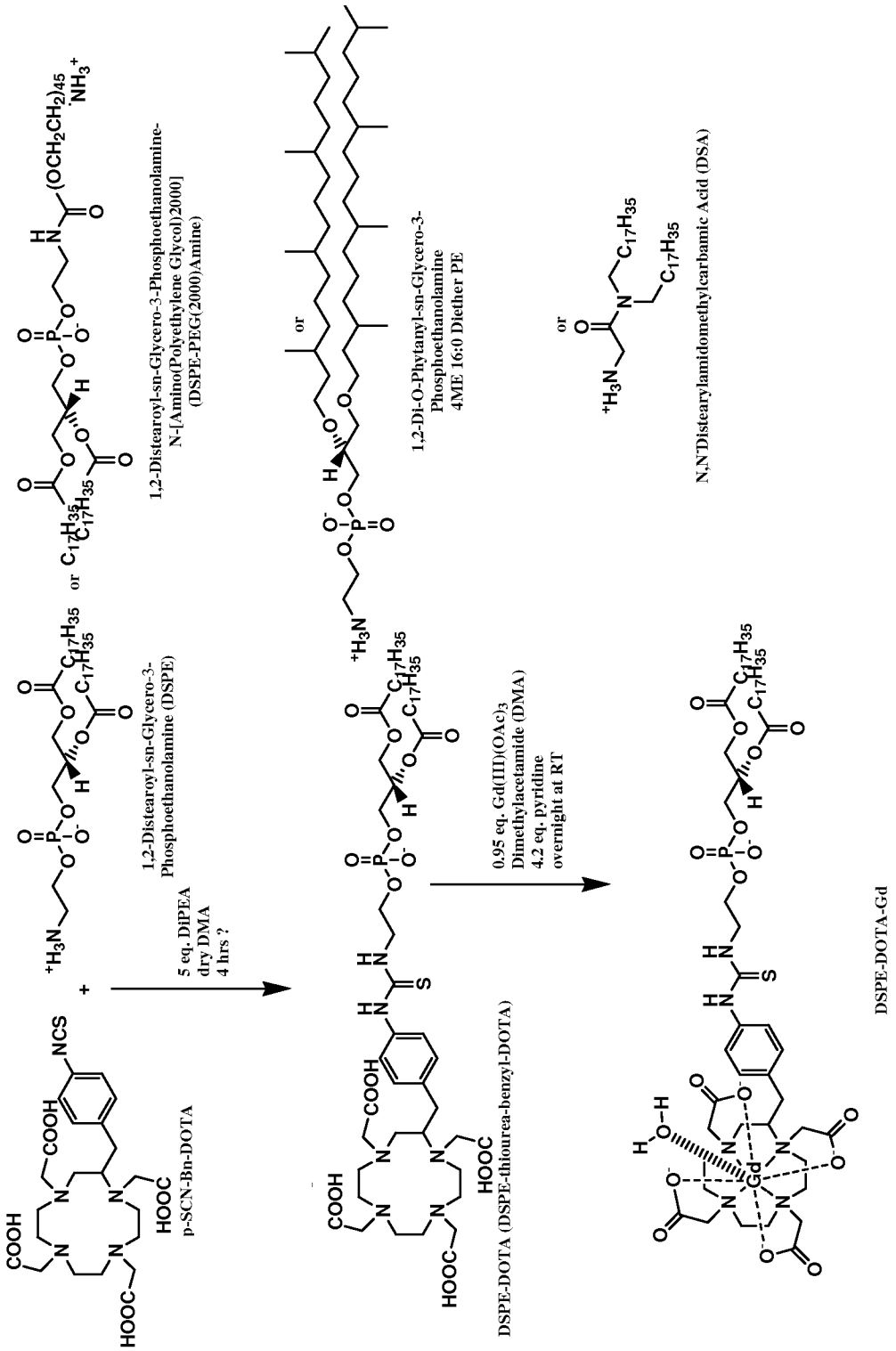
p-SCN-Bn-DOTA
1,2-Distearoyl-sn-Glycero-3-Phosphoethanolamine (DSPE)
or
1,2-Distearoyl-sn-Glycero-3-Phosphoethanolamine-N-[Amino(Polyethylene Glycol)2000] (DSPE-PEG(2000)Amine)
5 eq. DIPEA
dry DMA
4 hrs ?
DSPE-DOTA (DSPE-thiourea-benzyl-DOTA)
1,2-Di-O-Phytanyl-sn-Glycero-3-Phosphoethanolamine 4ME 16:0 Diether PE
0.95 eq. Gd(III)(OAc)3
Dimethylacetamide (DMA)
4.2 eq. pyridine
overnight at RT
N,N'Distearylamidomethylcarbamic Acid (DSA)
DSPE-DOTA-Gd

FIG. 12.